Cell-free Multi-Layered Collagen-Based Scaffolds Demonstrate Layer Specific Regeneration of Functional Osteochondral Tissue by 6 months in Caprine Joints

Authors:

Tanya J. Levingstone, BEng, MSc, PhD [1,2,3]

*Ashwanth Ramesh, MD[1,2,3]

*Robert T. Brady, MD[1,2,3]

Pieter A.J. Brama, DVM, PhD, MBA, DECVS, DRNVA [4]

Clodagh Kearney, MVB, DECVS [4]

John P. Gleeson, BA BAI, PhD, MIEI [1,2,3,5]

Fergal J. O'Brien, BA, BAI, PhD, FAS, CEng, FIEI [1,2,3]

Affiliations:

[1] Tissue Engineering Research Group, Department of Anatomy, Royal College of Surgeons in Ireland, 123 St. Stephen's Green, Dublin 2, Ireland.

[2] Trinity Centre for Bioengineering, Trinity College Dublin, Dublin 2, Ireland

[3] Advanced Materials and Bioengineering Research (AMBER) Centre, RCSI & TCD

[4] Section Veterinary Clinical Sciences, School of Veterinary Medicine, University College Dublin, Dublin, Ireland

[5] SurgaColl Technologies Ltd., Invent Centre, Dublin City University, Dublin, Ireland.

*Authors Ashwanth Ramesh and Robert Brady provided equal contributions to this work

Corresponding author:

Prof. Fergal O'Brien,

Department of Anatomy,

Royal College of Surgeons in Ireland,

123 St. Stephen's Green,

Telephone Number: +353 (0)1-402-2149

FAX Number: +353(0)1-402-2355

Email:fjobrien@rcsi.ie

Keywords: Tissue engineering, Collagen, *In vivo*, Osteochondral, Cartilage, Caprine model

Abstract

Developing repair strategies for osteochondral tissue presents complex challenges due to its interfacial nature and complex zonal structure, consisting of subchondral bone, intermediate calcified cartilage and the superficial cartilage regions. In this study, the long term ability of a multi-layered biomimetic collagen-based scaffold to repair osteochondral defects is investigated in a large animal model: namely critical sized lateral trochlear ridge and medial femoral condyle defects in the caprine stifle joint. The study thus presents the first data in a clinically applicable large animal model. Scaffold fixation and early integration was demonstrated at 2 weeks post implantation. Macroscopic analysis demonstrated improved healing in the multi-layered scaffold group compared to empty defects and a market approved synthetic polymer osteochondral scaffold groups at 6 and 12 months post implantation. Radiological analysis demonstrated superior subchondral bone formation in both defect sites in the multi-layered scaffold group as early as 3 months, with complete regeneration of subchondral bone by 12 months. Histological analysis confirmed the formation of well-structured subchondral trabecular bone and hyaline-like cartilage tissue in the multi-layered scaffold group by 12 months with restoration of the anatomical tidemark. Demonstration of improved healing following treatment with this natural polymer scaffold, through the recruitment of host cells with no requirement for pre-culture, shows the potential of this device for the treatment of patients presenting with osteochondal lesions.

1 Introduction

Osteochondral defects, resulting from traumatic injury or disease, are problematic within the clinical setting due to their limited potential for repair. A particular challenge presents due to the poor healing potential and avascular nature of cartilage and the interfacial nature of osteochondral tissue, with its complex zonal structure consisting of subchondral bone, intermediate calcified cartilage and the superficial cartilage regions (Matsiko et al, 2013). In the development of biomaterial and tissue engineering strategies for repairing this complex system, compositional, structural and mechanical factors all require consideration. While there have been recent advances in cell-based strategies and drug, gene and growth factor delivery systems for cartilage repair, these approaches are still limited by cost and the significant regulatory hurdles associated with clinical translation (Madry et al., 2014; Lee et

al., 2013). Thus the development of effective cell-free biomaterial-based approaches remains a critically important goal within the field of tissue engineering. The ideal biomaterial solution would achieve repair by encouraging the recruitment of cells from the underlying bone marrow and providing the physical and biochemical cues to direct these cells to regenerate the different regions of the joint.

Early attempts at the design of materials for the treatment of osteochondral defects focussed on the development of separate biomaterials for repair of the cartilage and bone regions which were fused together to create a bi-layered biomaterial. However, limited success has been achieved to date with this type of approach (Niederauer et al. 2000; O'Shea et al., 2008). In particular it is recognised that the calcified cartilage layer plays a significant role in preventing vascularisation of the overlying cartilage. The absence of this vital layer can result in bony ingrowth into the cartilage region (Hunziker et al. 2002). While a range of synthetic materials, including polycaprolactone (PCL) poly L-lactic acid (PLLA) and polyglycolic acid (PGA), have been used in cartilage repair applications with some success, natural biomaterials have a number of recognised advantages and thus may present an improved approach (Matsiko et al. 2013). In particular, collagen, which is present in most biological tissues, exhibits well documented biocompatibility and offers a number of advantages for use in tissue repair including ease of resorption *in vivo* without any resultant adverse response, greater cellular interaction due to the presence of ligands which may facilitate cell adhesion, and it can be co-polymerized with other biological materials to improve their bio-functionality. For example, collagen has been successfully combined with hydroxyapatite and chondroitin sulphate for bone repair and hyaluronic acid for cartilage repair (Tampieri et al. 2008; Zhou et al. 2011; Matsiko et al. 2012; Murphy et al. 2010; Farrell et al. 2006; Tierney & O'Brien 2009; Gleeson et al. 2010). Following this rationale, and based on the extensive experience with collagen-based biomaterials within our group, a multi-layered collagen-based scaffold with distinct but seamlessly integrated layers, that mimic the structure and composition of osteochondral tissue, has been developed (Levingstone et al. 2014; Gleeson et al. 2009). This scaffold is designed specifically for osteochondral defect repair and is fabricated using a novel 'iterative layering' freeze-drying technique to produce its seamlessly integrated layered structure (Fig. 1a). It consists of a bone layer composed of collagen type I and hydroxyapatite (HA) exhibiting osteoinductive properties and potential for bone repair

(Gleeson et al. 2010; Murphy et al. 2014; Lyons et al. 2014; David et al., 2015), a type I collagen and hyaluronic acid (HyA) intermediate layer representing the calcified cartilage region of native tissue, and a type I, type II collagen and HyA composite cartilaginous layer with excellent chondrogenic properties (Matsiko et al. 2012). Clinically, the scaffold is designed as an off-the-shelf cell-free biomaterial for press-fit implantation into an osteochondral defect site which, upon implantation into an osteochondral defect, enables infiltration of blood and cells from the host bone marrow through the seamlessly integrated multi-layered porous structure. The incorporated extracellular matrix macromolecules combined with biostructural and biomechanical properties are designed to encourage the proliferation and direct the differentiation of MSCs to produce bone, calcified cartilage and cartilage within the requisite regions. The regenerative potential of this multi-layered scaffold has been demonstrated *in vitro* (Levingstone et al., 2014) and this study presents the first data in a clinically applicable large animal model.

For clinical translation, *in vivo* assessment in a large animal model is required in order to truly evaluate the regenerative potential of any therapy which aims to eventually treat humans. The goat (caprine) stifle joint model presents an ideal model for cartilage repair as it closely matches the joint mechanics in the human situation (Patil et al. 2014). Additionally, the proportion of cartilage to subchondral bone and the subchondral bone consistency in goats is similar to humans (Ahern, 2009; Proffen et al. 2012). Identification of a suitable time scale for assessment also presents a challenge when developing materials for articular cartilage repair. In many cases, early repair with fibrous or fibro-cartilage repair tissue can appear promising, however, such tissue is mechanically unstable with degeneration likely over time (Falah et al. 2010) and thus evaluation at later points of up to 12 months post-implantation is ideally required (ASTM, 2010).

The objective of this study was thus to assess the ability of this novel multi-layered collagen-based scaffold to regenerate and repair osteochondral tissue in two surgically created critical sized osteochondral defects within the caprine stifle joint - the partial load bearing lateral trochlear ridge and the full load bearing medial femoral condyle - and to compare the *in vivo* response to that seen in an empty defect negative control and a market approved bi-layered synthetic polymer scaffold. The specific aims were firstly to assess scaffold fixation, cellular

infiltration and early tissue responses to the multi-layered scaffold at 2 weeks post implantation. Following on from this matrix deposition within the defect site was evaluated over time points of 3, 6 and 12 months to investigate if the biochemical and biostructural properties of this multi-layered scaffold enable regeneration of superficial articular cartilage, intermediate calcified cartilage and deep subchondral bone, with a zonal architecture similar to that of native osteochondral tissue.

2 Materials and methods

2.1 Fabrication of multi-layered scaffolds

Multi-layered scaffolds were fabricated using a unique iterative layering fabrication method developed in our lab (Levingstone et al. 2014) (Fig. 1a). Briefly, this process involved fabrication of an initial bone layer by blending type I collagen (Col1) [0.5% (w/v), Collagen Matrix Inc., NJ, USA] with hydroxyapatite (HA) [1% (w/v) Plasma Biotal, UK] at 4˚C for 4 hours to produce a Col1HA slurry, prior to freeze-drying in a stainless steel tray (60 mm x 60 mm internal diameter) at a freezing rate of 1 ˚/min to a final freezing temperature of -40˚C (Gleeson et al. 2010). Following freeze-drying the scaffold was cross-linked using 1-ethyl-3-(3-dimethylaminopropyl) carbodiimide (EDAC)/N-hydroxysuccinimide (NHS) (Sigma–Aldrich, Arklow, Ireland) at a concentration of 6 mM EDAC g^{-1} of collagen, and a 5:2 M ratio of EDAC:NHS for 2 hours at room temperature (Haugh et al. 2011). The intermediate layer slurry, consisting of Col1 [0.5% (w/v)], and hyaluronic acid sodium salt derived from streptococcus equi. (HyA) [0.05% (w/v), Sigma–Aldrich, Arklow, Ireland] was then added on top of the hydrated bone layer scaffold with freeze-drying repeated as before. Finally, the cartilage layer slurry, consisting of Col1 [0.25% (w/v)], type II collagen (Col2) [0.25% (w/v) porcine type 2 collagen, Biom'up, Lyon, France] and HyA [0.05% (w/v], was added and the process of freeze-drying was repeated again as described previously, incorporating prolonged freezing and drying steps to ensure optimal freeze-drying of the multi-layered construct. Following freeze-drying, the scaffolds were dehydrothermally (DHT) cross-linked in a vacuum oven (VacuCell, MMM, Germany) at 105°C and a pressure of 50 mTorr for 24 hours to generate cross-links through a condensation reaction and also sterilise the multi-layered scaffold sheet. Cylindrical scaffold plugs were cut to a diameter of 7 mm and a depth of 6 mm in order to provide a

158 secure press-fit on implantation. Finally, the plugs were EDAC cross-linked again under sterile
159 conditions as described previously.
160
161 **2.2 Study design**
162 *In vivo* assessment was carried out in a bi-lateral goat stifle joint model under ethical approval
163 (University College Dublin - AREC-P-11-31) and an animal licence granted by the Irish
164 Government Department of Health (B100/4317). A total of 19 adult female goats (2-3 years
165 old) were divided into 4 groups for assessment: 2 week and 3, 6 and 12 month post-
166 implantation with n numbers based on power analysis to provide an n=7 for the multi-layered
167 scaffold group as per Table 1. Surgeries and analysis for 2 week time points were carried out
168 first to assess surgical approach, scaffold fixation and early *in vivo* response. Following
169 positive findings at this early time point, the remaining 3, 6 and 12 month surgeries were
170 carried out. Surgeries were carried out bi-laterally with two defect sites created per stifle
171 joint, one on the lateral trochlear ridge and one on the medial femoral condyle (Fig. 1b and
172 c), with both sites within the same joint receiving the same treatment as per the treatment
173 plan set out in Table 1.
174
175 **2.3 Surgical procedure and scaffold implantation in caprine stifles**
176 The goats were sedated using Diazepam (0.3-0.4 mg/kg IV) and Butorphanol (0.2 mg/kg IV).
177 An epidural was administered using morphine (0.2 mg/kg) together with Bupivicaine (0.25-
178 0.35mg/kg). Following placement of an intravenous catheter, anaesthesia was induced with
179 propofol to effect (max dose 4mg/kg IV). Anaesthesia was maintained on isoflurane with
180 ventilation to maintain normal end tidal CO_2 between 4.6 and 6kPa. Isotonic fluids were
181 provided at 10ml/kg/hr. The goats were placed in dorsal recumbency and an arthrotomy of
182 each stifle joint was then performed using the lateral para-patellar approach. Two critical
183 sized defects (Jackson et al., 2001), 6 mm in diameter x 6 mm in depth, were created per stifle
184 joint, and one on the lateral trochlear ridge and one on the medial femoral condyle. Drilling
185 was performed using a hand drill to minimise heat production, with a 6 mm pointed drill bit
186 followed by a custom 6 mm flattened drill bit and drill sleeve to provide a uniform defect with
187 flattened bottom and controlled depth. The joint was flushed with normal saline and the stifle
188 joints were assigned to one of the three treatment groups: 1) empty defect, 2) multi-layered

scaffold, 3) bi-layered synthetic polymer scaffold (Trufit, Smith & Nephew, MA, USA). Both scaffold types were "press-fit" into the defect sites. The synthetic polymer scaffold was press-fit in place in accordance with the manufacturers' guidelines. Routine closure of the joint capsule, subcutaneous tissues and skin was then carried out. Morphine (0.1 – 0.2 mg/kg IM) and non-steroidal anti-inflammatory drugs (NSAIDs) [Carprofen (1.5 - 2.5 mg/kg subcutaneously) (Rimadyl), Zoetis, New Jersey, USA] were administered at the end of anaesthesia.

Following surgery, goats were housed in small indoor pens to allow skin incisions to heal and were allowed full weight bearing. During this period the animals were closely monitored to ensure adequate analgesia. NSAIDs and antibiotics [Amoxicillin (Noroclav), Norbook Laboratories Ltd; Corby, UK] were administered for 5 days post-surgery. Two weeks post-operatively, following removal of sutures, animals were let out to pasture for the remainder of the study period. Euthanasia was carried out at the 2 week and 3, 6 and 12 month time points with an overdose of sodium pentobarbital and stifle joints were harvested.

2.4 Macroscopic assessment of the level of repair at defect sites

Post euthanasia, the joints were opened and the defect site and surrounding joint tissues were examined. Synovial fluid was aspirated and inspected. Photographs of the defect sites were taken and three independent assessors who were blinded to the treatment groups assessed the quality of repair and regeneration using a macroscopic evaluation tool (Getgood et al. 2012) (Table 2). Osteochondral segments containing the defect sites surrounding by a margin of approximately 5 mm were subsequently resected and fixed in 10% formalin prior to further analysis.

2.5 Micro-computed tomography evaluation of subchondral bone formation

Micro-computed tomography (micro-CT) analysis was performed on all samples using a Scanco Medical 40 Micro-CT (Bassersdorf, Switzerland) with 70 kVP X-ray source and 112 µA (resolution of ~36 µm) in order to assess the quantity and structure of the new bone formed within the defect site. A constrained Gaussian filter was applied to partly suppress noise (filter width (0.8) and filter support (1)). Three-dimensional reconstructions were performed using

the Image-J and Bone-J software (public domain software developed by Wayne Rasband in the National Institute of Health, Maryland, USA) (Schneider et al. 2012) and a volume of interest (VOI) was defined within the subchondral bone region of the defect site. Subchondral bone repair was expressed as percentage bone volume over the total volume (% BV/TV).

2.6 Histological assessment of the level of repair at defect sites

Specimens were decalcified using 15% ethylenediaminetetraacetic acid (pH of 7.4) (EDTA, Fluka BioChemika, Sigma-Aldrich, Arklow, Ireland), then processed using an automated tissue processor (ASP300, Leica, Germany) before being embedded in paraffin wax blocks. Subsequently, 10 µm sections were then cut using a rotary microtome (Microsystems GmbH, Germany), and mounted on L-polylysine coated glass slides (Thermo Scientific, MenzelGmnh & Co KG, Germany). Following dewaxing, sections were stained histologically following standard protocols in order to assess, the quantity and quality of repair tissue and integration with native tissue. Specifically, haematoxylin and eosin (H&E) was used to assess cell arrangement and morphology and tissue formation and integration; Masson's trichrome was used to assess the collagen formation within the cartilage region and bone formation with the subchondral bone region; and safranin-O with fast green counterstain was used to assess the presence of glycosaminoglycan within the repair tissue in the cartilage region. Images from each specimen were acquired using bright-field microscopy and digitised (Nikon Microscope Eclipse 90i with NIS Elements software v3.06, Nikon Instruments Europe, The Netherlands). The thickness of the cartilage layer (measured from the joint surface to the tidemark) in the trochlear ridge (n=3) and medial condyle (n=3) defect sites was compared to normal cartilage thickness adjacent to the defect area. Qualitative histological scoring was carried out independently by a certified histopathologist under blinded conditions using a modification of the histological scoring system developed by O'Driscoll (O'Driscoll et al. 1986) which has been previously validated for the assessment of articular cartilage repair (Rutget et al. 2010; Moojen et al. 2002) while also allowing assessment of the subchondral bone. The scoring system was used to provide a comprehensive evaluation of repair within the osteochondral defect site using six categories (I) the nature of cartilage repair tissue (II) structural characteristics, (III) freedom from cellular changes or degradation, (IV) freedom

from degradation changes in articular cartilage (V) reconstitution of subchondral bone and (VI) safranin-O staining, and has a maximum possible score of 28 (Table 3).

2.7 Statistical analysis

Data from the *in vivo* experiments were analysed with two-way ANOVA and Bonferroni post hoc analysis for multiple comparisons to look for any statistical differences among the three groups with an alpha value set at $p<0.05$. Data was analysed using GraphPad Prism version 5.00 for Windows (GraphPad Software, San Diego California USA).

3 Results

3.1 Clinical observations after scaffold implantation

During surgery, scaffolds were successfully implanted using the press-fit implantation technique and were seen to fill with blood on implantation (Fig. 2a). All animals recovered well post operatively and within 5 days ambulated freely with no signs of distress or limping for the duration of the study. There were no post-operative complications up to the 12 month time point.

3.2 Macroscopic assessment of defect repair

On opening of the joints, gross macroscopic visual evaluation of the repair tissue was carried out. Synovial fluid was found to be straw coloured, clear and normal in all cases. There was no evidence of negative inflammatory responses or degenerative changes, construct delamination or migration into the joint cavity in the treated joints based on visual assessment at the time of retrieval. At 2 weeks post implantation, macroscopic assessment enabled visualisation of the scaffold within the defect site and demonstrated successful fixation of the scaffold using the press-fit implantation method (Fig. 2b and c). At 3 months, some level of defect fill was observed in both defect sites in the empty and multi-layered scaffold groups, with signs of repair tissue present within the defect site. By 6 months, both defect sites in the multi-layered scaffold group showed evidence of smooth cartilage-like tissue with good integration of the repair tissue to the surrounding healthy tissue within the defect site, whereas incomplete defect fill and limited tissue integration was observed in the

synthetic polymer scaffold group. At 12 months, the defect sites in the multi-layered scaffold group showed improved articular cartilage regeneration and repair compared to empty or the synthetic polymer scaffold groups (Fig. 3a and c). In this group, cartilage was hyaline-like in appearance, with complete integration of the newly formed cartilage into the surrounding healthy tissue. Additionally, there was complete defect fill, and the colour of the cartilage within the defects was close to that of the surrounding native tissue. In contrast, in the empty defect and the synthetic polymer scaffold groups defect sites displayed signs of incomplete healing. Notably, in the medial condyle treated with the synthetic polymer scaffold there was fibrous-like tissue present within the defect and the presence of large fissures with the repair tissue was observed. Noticeable depressions were observed in the central region of the defect site in the empty defect group.

Gross morphological scores were consistent with findings of the visual evaluation (Fig. 3b and d). At 3 months, there was no statistically significant difference between scores for the empty defect group in the trochlear ridge and medial condyle defect sites compared to the multi-layered scaffold group. At 6 months, the empty defect trochlear ridge group displayed significantly higher scores when compared to multi-layered ($p<0.01$) and the synthetic polymer scaffold ($p<0.001$). However, higher scores were seen in the multi-layered scaffold in the medial condyle defect sites compared to empty and the synthetic polymer scaffold groups; with significance found between the multi-layered scaffold group and the synthetic polymer scaffold group ($p<0.01$). At the final 12 month evaluation, the trochlear ridge defect site in the multi-layered scaffold group showed greater levels of repair compared to empty ($p<0.05$) and the synthetic polymer scaffold ($p<0.01$) groups (Fig. 3b). A similar trend was observed in the medial condyle with the multi-layered scaffold group demonstrating significantly higher gross morphological scores compared to empty ($p<0.001$) and the synthetic polymer scaffold group ($p<0.01$) (Fig. 3d). Overall, these results indicate that the gross morphological appearance was deemed to be superior by three independent assessors in both defect sites in the multi-layered group compared to the empty and synthetic polymer scaffold groups at the final 12 month time point.

3.3 Micro-computed tomography evaluation of subchondral bone formation

Following visual assessment of repair tissue, levels of subchondral bone formation were investigated using micro-CT. Analysis of 2D projections demonstrated superior levels of subchondral bone formation in both defect sites in the multi-layered scaffold group starting as early as 3 months, with improved levels of subchondral bone repair at 6 months and complete regeneration of subchondral bone by 12 months (Fig. 4a and c). In contrast, the empty group medial condyle and trochlear ridge defect sites showed minimal signs of healing at the 3 and 6 month time points, with some subchondral bone repair observed by 12 months post-op. In the synthetic polymer scaffold group, while there was some variability, as early as 6 months, there was evidence of osteolysis resulting in defect widening in both defect sites in the synthetic polymer scaffold group. As a consequence of the osteolysis, in some cases the synthetic polymer scaffold groups presented with cavities that persisted up to 12 months and displayed minimal signs of subchondral bone formation. These findings were confirmed through quantification of the bone volume within the defect site with significantly higher BV/TV values in the multi-layered scaffold group trochlear ridge and medial condyle defect sites relative to the empty and the synthetic polymer scaffold groups at 6 months ($p<0.001$) and 12 months (trochlear ridge ($p<0.001$) and medial condyle ($p<0.05$).

3.4 Microscopic assessment of repair within defect sites

Histological assessment of repair supported the macroscopic and micro-CT findings with defect repair occurring in the multi-layered scaffold group over the 3, 6 and 12 month time points. The multi-layered scaffold group displayed evidence of newly formed repair tissue which integrated into the surrounding healthy cartilage by 12 months in both defect sites as evidenced by the haematoxylin and eosin (H&E) staining (Fig. 5a and b) and hyaline-like cartilage formation as demonstrated by safranin-O staining (Fig. 6a and b). The structure of the cartilage repair tissue in the multi-layered group had an immature fibrous appearance at 6 months but by 12 months showed strong sulphated GAG staining and a more hyaline-like appearance (Fig. 7a and b). Cells within the cartilage region displayed a rounded morphology and were found residing within lacunae and with alignment typical of native cartilage (Fig. 7a and 7b). The newly formed hyaline-like cartilage tissue was supported by a well-structured subchondral trabecular bone that was hard to distinguish from the surrounding healthy bone. Most notably, tidemark formation was observed with no evidence of any bony invasion past

the calcified cartilage layer into the regenerated cartilage layer (Fig. 7c). In comparison, the trochlear ridge and medial condyle defects treated with the synthetic polymer scaffold showed loss of subchondral bone with resorption of surrounding healthy osseous tissue at 6 and 12 months post op. There was evidence of cavity formation in the subchondral bone, causing the overlying cartilage-like tissue to subside into the defect. The nature of the cartilage tissue was predominantly fibrocartilage with varying amounts of primarily woven bone and fibrous connective tissue. Furthermore, remnants of the scaffolds were still visible at 6 and 12 months (Fig. 7d, e and f), and there was a complete failure of integration of the scaffold with the surrounding healthy tissue. At 12 months, in the empty group, the trochlear ridge and medial condyle defects were filled with poor quality fibrous tissue with poor regeneration of the individual cartilage, calcified cartilage and bone layers of the osteochondral defect.

Regeneration of cartilage and bone tissue in the osteochondral defect was quantified using a histological evaluation tool based on the O'Driscoll scoring system to allow assessment of the articular cartilage and also the subchondral bone (Rutget et al. 2010; Moojen et al. 2002; Getgood et al. 2012). As early as 3 months, the multi-layered scaffold group performed better with higher histological scores compared to the empty group; although this was only significant in the medial condyle defects. At 6 months, the histological scores for the trochlear ridge and medial condyle defects were comparable between all treatment groups. However, and perhaps most importantly, at 12 months, both the trochlear ridge and medial condyle defect sites treated with the multi-layered scaffold demonstrated improved repair as evidenced by higher histological scores compared to the empty and synthetic polymer scaffold groups ($p<0.05$) (Fig. 8a and b). Additionally, at this time point the nature of the tissue above the tidemark in the multi-layered group was predominantly hyaline as evidenced by positive safranin-O staining. Over the 12 months study period, there was evidence of the maturation of the cartilaginous tissue in the multi-layered scaffold group compared to the empty and synthetic polymer scaffold groups. In addition, there was demonstrated integration with the surrounding healthy cartilage tissue and reconstitution of subchondral bone without any signs of bone overgrowth beyond the tidemark were demonstrated. Consequently, the multi-layered group achieved significantly better histological scores ($p<0.05$) compared to the empty and synthetic polymer scaffold groups.

3.5 Microscopic assessment of cartilage thickness at defect sites

The findings of the histological evaluation were reflected in the cartilage thickness analysis where the multi-layered scaffold group showed greater cartilage thickness compared to the empty ($p<0.01$) and the synthetic polymer scaffold groups ($p<0.05$) at 6 months and 12 months respectively (Fig. 8c). The cartilage thickness at 3 months was difficult to measure due to lack of a clearly visible tidemark layer in the defects, therefore only 6 and 12 month measurements were taken with both medial condyle and trochlear ridge sites being analysed together. At 6 months, the multi-layered group demonstrated greater cartilage thickness (213 μm); this was significant compared to empty (96 μm, $p<0.01$) and the synthetic polymer scaffold (140 μm, $p<0.05$) groups. At 12 months, an increase in cartilage thickness values were seen in the multi-layered group (238 μm) compared to empty (98 μm, $p<0.01$) and the synthetic polymer scaffold (66 μm $p<0.05$) groups. Although thickness values appeared lower than normal cartilage thickness (256 μm), this was not significant at either time point. Most notably, the cartilage thickness in the synthetic polymer scaffold group displayed a reduction from 6 months to 12 months compared to the defects treated with the multi-layered scaffold.

4 Discussion

This study demonstrates the significant clinical potential of this multi-layered scaffold as an off-the-shelf biomaterial solution for osteochondral defect repair and demonstrates the potential for a positive impact in the treatment of patients presenting with osteochondal lesions. The development of advanced biomaterial-based strategies for osteochondral defect repair is of critical importance in clinical orthopaedics in order to address a major clinical need. To address this, a novel multi-layered collagen-based osteochondral defect repair scaffold, consisting of three distinct but seamlessly integrated layers designed to mimic the stratified composition of native osteochondral tissue, has been developed within our lab (Levingstone et al. 2014). The objectives of this study were therefore to evaluate the ability of this novel multi-layered scaffold to regenerate and repair osteochondral tissue within two surgically created critical sized osteochondral defects in the caprine stifle joint, the medial femoral condyle and lateral trochlear ridge, and to compare the *in vivo* response to that seen in an empty defect at 3, 6 and 12 month time points and market approved synthetic polymer

scaffold at 6 and 12 months. Scaffold fixation and early integration was demonstrated at 2 weeks post implantation. Macroscopic analysis demonstrated improved healing in the multi-layered scaffold group compared to empty defects and a market approved synthetic polymer osteochondral scaffold groups at 6 and 12 months post implantation. Radiological analysis demonstrated superior subchondral bone formation in both defect sites in the multi-layered scaffold group as early as 3 months, with complete regeneration of subchondral bone by 12 months. Histological analysis confirmed the formation of well-structured subchondral trabecular bone and hyaline-like cartilage tissue in the multi-layered scaffold group by 12 months with restoration of the anatomical tidemark.

A significant outcome for this study was that there were no joint related adverse events or post-operative complications with all animals recovering well. This demonstrates the safety of the multi-layered scaffold and further validates the surgical approach used. While promising *in vitro* results have already been demonstrated, assessment in large animals is desirable in order to truly evaluate the regenerative capacity of this scaffold. While numerous large animal models are used in the literature, the caprine stifle joint defect model is widely accepted as an ideal large animal model for assessment of the efficacy of strategies for cartilage repair, due to the thickness of the cartilage present on the articulating surfaces and also the anatomical similarity of the stifle joint to human knee joint (Ahern et al. 2009; Proffen et al. 2012). The use of two defect sites within the stifle joint provides the opportunity to assess tissue regeneration in two different loading environments, the partially loaded trochlear ridge and fully loaded femoral condyle. Comparison of joint forces has demonstrated that peak contact pressures in goat knees are comparable to those generated in human knees (Patil, 2014). The goat model also allows similar surgical techniques to those used in humans. The 6 mm x 6 mm size defect used was also validated with minimal tissue regeneration observed in the empty defect groups, in line with findings from previous studies (Jackson et al. 2001). Infiltration of blood and cells into the empty defect from the subchondral bone led to fibrous tissue formation at early time points and good early macroscopic scores, however, it is evident from radiological and histological assessment that this does not translate to repair of the cartilage and subchondral bone at later time points. Jackson et al. (2001) reported widening of the defect walls in an empty defect created in the

medial femoral condyle of a goat knee joint by 6 weeks post op, resorption of the bone surrounding the defect by 26 weeks and sclerotic bone at the defect edges by 52 week post op. Similar findings were observed in this study and thus it is clear that without intervention, complete healing of the osteochondral defect site cannot be achieved.

There are two defect sites commonly used in the literature, the lateral trochlear ridge and medial femoral condyle (Niederauer et al. 2000; Orth et al. 2013). Levels of repair are reported to vary between the two defect sites and the ideal site for assessment of the efficacy of materials for cartilage repair is still not clear. Orth et al. (2013) reported improved osteochondral repair in the trochlear ridge compared to the medial condyle at 6 months in an ovine model, whereas Niederauer et al. (2000) reported improved healing in the medial condyle compared to the trochlear at 6 months post implantation of an osteochondral defect repair scaffold. In this study a direct comparison between the tissue regeneration observed in the two sites was carried out. In the empty defect group, while BV/TV values were the same for both sites, macroscopic and histological scoring indicated that greater levels of spontaneous repair occurred in the trochlear ridge. In the multi-layered scaffold group macroscopic scoring and BV/TV values were marginally higher in the trochlear ridge defect site than the medial condyle, however, no statistical differences were found between the two sites. Thus while differences in loading and spontaneous repair exist between the two sites, when treated with the multi-layered scaffold similar levels of repair can be achieved.

Retention of the scaffold within the defect site was demonstrated at 2 weeks post implantation, thus validating the press-fit fixation method without the use of a cast or splint mechanism to stabilise the joint. Several scaffold fixation strategies have been investigated in the literature, including gluing and suturing, but negative inflammatory responses (van Susante et al. 1999) and degradation changes due to suture trauma (Hunziker et al. 2008) have been reported. As the defect sites utilised in this model are both load-bearing, the scaffold would have been subjected to compressive forces during the study. Histological analysis at 2 weeks demonstrated that the scaffold has sufficient mechanical properties to remain within the defect site flush with the articular surface (Fig. 2d). It was also evident that the multi-layered porous architecture in the scaffold was maintained in the *in vivo* environment thus permitting cell infiltration into the scaffold structure. Upon implantation, a

heterogeneous mixture of blood, immune, and precursor cells from the bone marrow enter into the defect site and infiltrate through the seamlessly integrated layers of the multi-layered scaffold. This was observed initially as a change in colour of the scaffold from white to red on implantation (Fig. 2a) and also demonstrated histologically (Fig. 2e, f and g). The results suggest that the infiltrating precursor cell population present is capable of differentiating to bone and cartilage forming cells, directed by the scaffold architecture and matrix macromolecules, resulting in repair of the surrounding tissues and, together with the immune cell population, remodelling and degradation of the implanted scaffold. This scaffold-mediated approach offers advantages over complex cell seeded tissue engineering strategies as it negates the requirement for costly and time consuming *ex vivo* cell expansion and cell seeding procedures.

Analysis of repair at the time points of 3, 6 and 12 months post-implantation demonstrated improved healing in the multi-layered scaffold group compared to the synthetic polymer scaffold or empty defect groups. Blinded macroscopic evaluation of repair tissue using a gross macroscopic scoring system indicated improved healing within the multi-layered scaffold group. While similar macroscopic scores were observed between the multi-layered scaffold and empty defect groups at 3 and 6 months, the multi-layered scaffold group exhibited improved healing over the synthetic polymer scaffold group at 6 months (Fig. 3b and d). Presence of a smooth white cartilaginous layer that appeared to be continuous with the surrounding healthy cartilage was observed in the trochlear ridge and medial condyle defect sites in the multi-layered scaffold group at 12 months with improved colour, and greater defect fill, integration and surface smoothness compared to the empty defect and synthetic polymer scaffold groups (Fig. 3a and c). Assessment of new bone formation using micro-CT demonstrated a clear trend showing superior levels of subchondral bone regeneration from 3 months to 12 months post surgery in the multi-layered group defects compared to empty group and synthetic polymer scaffold (Fig. 4). In the multi-layered scaffold groups similar levels of bone repair were observed in both defect sites at both 6 and 12 month time points, with average BV/TV values of 0.56 in the trochlear ridge and 0.53 in the medial condyle at 12 months. Comparison of the 2D micro-CT projections shows that early mineral deposition at 3 and 6 months undergoes remodelling with advanced stages of bone repair evident in the multi-layered scaffold group at 12 months (Fig. 4a and c). While some new bone formation

was observed in the empty defect group, repair remained incomplete up to 12 months post op. In the synthetic polymer scaffold group resorption of the osseous wall of the defect and defect widening was observed. Consequently, the synthetic polymer scaffold demonstrated lower bone volume (BV/TV) values compared to the multi-layered scaffold group.

Histological analysis confirmed the findings from micro-CT showing reconstruction of subchondral bone plate forming the tidemark and repair of the underlying bone in the multi-layered scaffold group with evidence of neovascularisation as early as 6 months (Fig. 5 and 6). Tidemark formation is essential in order to achieve long-term stability of the newly formed tissue; providing structural support to the overlying cartilaginous layer and also forming a natural boundary between vascularised subchondral bone and avascular articular cartilage to prevent bony overgrowth into the cartilaginous region of the defect site. Bony overgrowth has been linked with degenerative changes within the joint (Abarrategi et al. 2010) and is frequently observed following ACI procedures (Minas et al. 2005; Henderson et al. 2009) and resulting for other biomaterial approaches to osteochondral defect repair (Coburn et al. 2012). Assessment of repair tissue in the cartilaginous region in the multi-layered scaffold group showed the presence of fibro-cartilage tissue at 6 months with more hyaline-like cartilage being observed by 12 months post op (Fig. 7a and b). At both time points cells displayed a rounded morphology and were found residing within lacunae, characteristics typical of chondrocytes in native cartilage, and showed cellular alignment typical of cartilage with matrix staining positive for glycosaminoglycans (Fig. 7a and b). Quantification of repair through histological scoring confirmed improved repair within the multi-layered scaffold group than the empty defect or synthetic polymer scaffold groups (Fig. 8a and b).

Overall these results demonstrate that greater levels of repair resulted following treatment with the multi-layered scaffold than the synthetic polymer scaffold. Comparison of the composition and micro-structure of the scaffolds investigated here provides some explanation for the different responses observed *in vivo*. The multi-layered scaffold is composed of natural polymers, type I and type II collagen, hyaluronic acid (HyA) in addition to hydroxyapatite (HA). This has demonstrated significant potential *in vitro* to support chondrogenesis as well as *in vivo* healing by the collagen-HA bone layer (Gleeson et al. 2010; Lyons et al. 2014; Murphy et al. 2014; Matsiko et al. 2012). The main constituent of the

synthetic polymer scaffold is polyglycolic acid (PLGA), and while this material has been shown to support cartilage production *in vitro* (Niederauer et al. 2000), its chondroinductive properties have not been demonstrated. The bone region of the multi-layered scaffold provides a more favourable biomimetic environment as the mineral phase present is hydroxyapatite which is found in native bone, whereas the synthetic polymer scaffold contains calcium-sulfate. Differences in scaffold degradation properties may also significantly contribute to the repair responses observed in each group. While the multi-layered scaffold had fully resorbed by the 6 month time point, remnants of the synthetic polymer scaffold persisted (Fig. 7d, e and f). Collagen-based materials degrade via natural enzymatic processes involving proteases such as collagenases, resulting in degradation products such as oligomeric peptide and saccharide fragments, that do not negatively affect their local microenvironment (Pek et al. 2004). In contrast, synthetic polymers have shown less favourable responses *in vivo* with previous reports highlighting negative inflammatory processes as a result of the degradation products of synthetic polymers (Sittinger et al. 1999; Asawa et al, 2012; Lee et al. 2014). While a number of studies have reported clinical success using the synthetic polymer scaffold for osteochondral repair (Dhollander et al. 2012; Bekkers et al. 2013; Hindle et al. 2014; Joshi et al., 2012; Pearce et al. 2012), some concerns have been raised over the long term efficacy of this device Carmont et al. (2009); Verhaegen J et al. (2015) and Getgood et al. (2012). Polyglycolic acid (PLGA) degrades as a result of hydrolytic cleavage of ester bonds within the material leading to the release of acidic by-products including lactic acid and glycolic acid (Antheunis et al. 2010). Poor levels of tissue repair observed at 6 and 12 months within the synthetic polymer scaffold group can be attributed to this local acidic environment resulting from scaffold degradation. Similar findings have been reported previously by Asawa et al. (2012). Moreover, acid-sensitive bone structural components such as calcium phosphate may be weakened as a result, thus leading to the breakdown of bone tissue and the formation of bone cysts (Getgood et al. 2012). The recognised limitations of synthetic biomaterials for cartilage repair applications has led to a move to more natural materials, with recent osteochondral defect repair materials emerging onto the marketplace in Europe including Maioregen (Finceramica, Italy), a triphasic type I equine collagen osteochondral scaffold containing magnesium enriched hydroxyl appetite, and Agili C (Cartiheal, Israel) made from coralline aragonite.

Taken together, the results presented here demonstrate the effectiveness of this multi-layered collagen-based material in the treatment of focal osteochondral lesions and show an improved regenerative response following treatment with this collagen-based multi-layered scaffold in comparison to a market approved synthetic polymer scaffold. This study thus validates the use of this scaffold as an off-the-shelf cell-free therapeutic and demonstrates its potential for successful translation to the clinic. Due to its multi-layered structure, tailored compositional and biomechanical properties, this scaffold also provides an ideal platform for the development of advanced therapies for osteochondral defect repair and is ideally suited for the delivery of a range of complex biomolecules not limited to just cells but also for the delivery of growth factors or as gene-activated matrices to promote enhanced tissue repair. Such approaches have already been demonstrated with similar collagen-based scaffolds from our group (Castaño et al. 2015; Raftery et al. 2015; Quinlan et al. 2015; Tierney et al. 2013; Matsiko et al. 2015). While such advanced treatment systems still have a way to go before reaching the clinic, strategies such as these could thus lead to successful healing in the treatment of areas of large scale damage to the articular surface in the future.

5 Conclusion

Overall the results of this study have shown successful, *in vivo* repair and regeneration of the subchondral bone and overlying superficial cartilage with restoration of the tidemark within critical sized caprine osteochondral defects in 2 distinct joint locations, following implantation of a novel multi-layered collagen-based osteochondral defect repair scaffold. Evaluation of repair at 3, 6 and 12 months demonstrated that the biochemical and biostructural properties of this multi-layered scaffold enabled improved regeneration over a bi-layered synthetic polymer scaffold, with a zonal architecture similar to that of native osteochondral tissue observed in the multi-layered scaffold groups at 12 months. Results demonstrated greater levels of repair macroscopically, radiographically and microscopically, with quantification demonstrating increased cartilage thickness and superior levels of subchondral bone formation in the multi-layered scaffold group compared to empty and synthetic polymer scaffold groups. Taken together these results show the importance of biomaterial, biochemical and biostructural properties in the design of materials for tissue repair.

Acknowledgements

The authors acknowledge Enterprise Ireland Proof of Concept Award (PC/2007/331) Commercialisation Fund Technology Development Award (CFTD/2009/0104) and Innovation Partnership Award (IP/2014/0162) and Science Foundation Ireland (SFI)/ Health Research Board (HRB) Translational Research Award (TRA/2011/19) for funding.

The authors wish to acknowledge Dr. Aurelie Fabre, St. Vincents' Hospital Dublin for assistance with histological scoring.

Conflict of Interest

Authors JP Gleeson, TJ Levingstone and FJ O'Brien hold IP with a commercial product of related composition to the collagen-based scaffolds used in this study.

References

Abarrategi A, Lopiz-Morales Y, Ramos V, Civantos A, Lopez-Duran L, Marco Fet al. Chitosan scaffolds for osteochondral tissue regeneration. J Biomed Mater Res A. 2010;95(4):1132-41.

Ahern BJ, Parvizi J, Boston R, Schaer TP. Preclinical animal models in single site cartilage defect testing: a systematic review. Osteoarthritis Cartilage. 2009;17(6):705-13.

Antheunis H, van der Meer JC, de Geus M, Heise A, Koning CE. Autocatalytic equation describing the change in molecular weight during hydrolytic degradation of aliphatic polyesters. Biomacromolecules 2010;11(4):1118–24.

Asawa Y, Sakamoto T, Komura M, Watanabe M, Nishizawa S, Takazawa Y, et al. Early stage foreign body reaction against biodegradable polymer scaffolds affects tissue regeneration during the autologous transplantation of tissue-engineered cartilage in the canine model, Cell Transplant. 2012;21(7):1431-1442.

ASTM. Standard Guide for *in vivo* Assessment of implantable devices intended to repair or regenerate articular cartilage. American Society for Testing and Materials. 2010.

626

627 Bedi A, Foo LF, Williams RJ, Potter HG. The Maturation of Synthetic Scaffolds for
628 Osteochondral Donor Sites of the Knee: An MRI and T2-Mapping Analysis.
629 Cartilage. 2010;1(1):20-8.

630

631 Bekkers JEJ, Bartels LW, Vincken KL, Dhert WJA, Creemers LB, Saris DBF. Articular cartilage
632 evaluation after TruFit plug implantation analyzed by delayed gadolinium-enhanced MRI of
633 cartilage (dGEMRIC). Am J Sports Med. 2013;41(6):1290-5.

634

635 Carmont MR, Carey-Smith R, Saithna A, Dhillon M, Thompson P, Spalding T. Delayed
636 incorporation of a TruFit plug: perseverance is recommended. Arthroscopy. 2009;25(7):810-
637 4.

638

639 Castaño IM, Curtin CM, Shaw G, Murphy JM, Duffy GP, O'Brien FJ. A novel collagen-
640 nanohydroxyapatite microRNA-activated scaffold for tissue engineering applications capable
641 of efficient delivery of both miR-mimics and antagomiRs to human mesenchymal stem cells.
642 J Control Release. 2015;28(200):42-51.

643

644 Coburn JM, Gibson M, Monagle S, Patterson Z, Elisseeff JH. Bioinspired nanofibers support
645 chondrogenesis for articular cartilage repair. Proc Natl Acad Sci. 2012;109(25): 10012-7.

646

647 David F, Levingstone TJ, Scheeweiss W, de Swarte M, Jahns H, Gleeson JP et al. Enhanced bone
648 healing using collagen-hydroxyapatite scaffold implantation in the treatment of a large
649 multiloculated mandibular aneurysmal bone cyst in a Thoroughbred filly. J Tissue Eng Regen
650 Med. 2015; doi: 10.1002/term.2006. [Epub ahead of print]

651

652 Dhollander AAM, Liekens K, Almqvist KF, Verdonk R, Lambrecht S, Elewaut D, et al. A pilot
653 study of the use of an osteochondral scaffold plug for cartilage repair in the knee and how to
654 deal with early clinical failures. Arthroscopy. 2012;28(2):225-33.

655

656 Falah M, Nierenberg G, Soudry M, Hayden M, Volpin G, 2010. Treatment of articular cartilage
657 lesions of the knee. Int Ortho. 2010;34(5):621–630

Farrell E, O'Brien FJ, Doyle P, Fischer J, Yannas I, Harley BA, et al. A collagen-glycosaminoglycan scaffold supports adult rat mesenchymal stem cell differentiation along osteogenic and chondrogenic routes. Tissue Eng. 2006;12(3):459–468

Getgood A, Kew SJ, Brooks R, Aberman H, Simon T, Lynn AK, et al. Evaluation of early-stage osteochondral defect repair using a biphasic scaffold based on a collagen-glycosaminoglycan biopolymer in a caprine model. Knee. 2012;19:422-430.

Gleeson JP, Levingstone TJ, O'Brien FJ. Layered scaffold suitable for osteochondral defect repair. Patent WO2010/084481, 2009.

Gleeson JP, Plunkett NA, O'Brien FJ. Addition of hydroxyapatite improves stiffness, interconnectivity and osteogenic potential of a highly porous collagen-based scaffold for bone tissue regeneration. Eur Cell Mater. 2010;20:218-30.

Haugh MG, Murphy CM, McKiernan RC, Altenbuchner C, O'Brien FJ. Crosslinking and mechanical properties significantly influence cell attachment, proliferation, and migration within collagen glycosaminoglycan scaffolds. Tissue Eng Part A, 2011;17(9-10):1201–1208

Henderson IJP, La Valette DP. Subchondral bone overgrowth in the presence of full-thickness cartilage defects in the knee. Knee. 2005;12:435-440.

Hindle P, Hendry JL, Keating JF, Biant LC. Autologous osteochondral mosaicplasty or TruFit plugs for cartilage repair. Knee Surg Sports Traumatol Arthrosc. 2014;22(6):1235-40.

Hunziker, EB. Articular cartilage repair: basic science and clinical progress. A review of the current status and prospects. Osteoarthritis and cartilage / OARS, Osteoarthritis Research Society, 2002;10(6):432–63.

Hunziker EB, Stahli A. Surgical suturing of articular cartilage induces osteoarthritis-like changes. Osteoarthritis Cartilage.2008;16:1067–1073.

690
691 Jackson DW, Lalor PA, Aberman HM , Simon TM. Spontaneous Repair of Full-Thickness
692 Defects of Articular Cartilage in a Goat Model A Preliminary Study, J Bone Joint Surg
693 Am, 2001;83 (1):53 -53
694
695 Joshi N, Reverte-Vinaixa M, Diaz-Ferreiro EW, DominguezOronoz R. Synthetic resorbable
696 scaffolds for the treatment of isolated patellofemoral cartilage defects in young patients:
697 magnetic resonance imaging and clinical evaluation. Am J Sports Med. 2012;40(6):1289-95.
698
699 Lee YR, Lee YH, Kim KH, Im SA, Lee CK.. Induction of potent antigen-specific cytotoxic T cell
700 response by PLGA-nanoparticles containing antigen and TLR agonist. Immune network.
701 2013;13(1): 30-33.
702
703 Lee JK, Respontea D, Cissella DD, Hua JC, Noltab JA, Athanasiou KA. Clinical translation of stem
704 cells: insight for cartilage therapies Critical Reviews in Biotechnology. 2014; 34(1):89-100
705
706 Levingstone TJ, Matsiko A, Dickson GR, O'Brien FJ, Gleeson JP. A biomimetic multi-layered
707 collagen-based scaffold for osteochondral repair. Acta Biomater. 2014;10(5):1996-2004.
708
709 Levingstone TJ, Thompson E, Matsiko A, Gleeson JP, O'Brien FJ. Multi-Layered Collagen-Based
710 Scaffolds for Osteochondral Defect Repair in Rabbits (2015)
711
712 Lyons FG, Gleeson JP, Partap S, Coghlan K, O'Brien FJ. Novel microhydroxyapatite particles in
713 a collagen scaffold: a bioactive bone void filler? Clin Orthop Relat R. 2014;472(4):1318-1328
714
715 Madry H, Alini M, Stoddart MJ, Evans C, Miclau T, Steiner S. Barriers and strategies for the
716 clinical translation of advanced orthopaedic tissue engineering protocols, European Cells and
717 Materials. 2014;27s:17-21
718
719 Matsiko A, Levingstone TJ, O'Brien FJ, Gleeson JP. Addition of hyaluronic acid improves
720 cellular infiltration and promotes early-stage chondrogenesis in a collagen-based scaffold for
721 cartilage tissue engineering J Mech Behav Biomed Mater. 2012;11:41-52.

722

723 Matsiko A, Levingstone TJ, O'Brien FJ. Advanced Strategies for Articular Cartilage Defect
724 Repair. Materials. 2013;6:637-668.
725
726 Matsiko A, Levingstone TJ, Gleeson JP, O'Brien FJ. Incorporation of TGF-Beta 3 within
727 Collagen–Hyaluronic Acid Scaffolds Improves their Chondrogenic Potential. Adv Healthc
728 Mater. 2015;4(8):1175-9.
729
730 Minas T, Gomoll AH, Rosenberger R, Royce RO, Bryant T. Increased failure rate of autologous
731 chondrocyte implantation after previous treatment with marrow stimulation techniques. Am.
732 J. Sport Med. 2009:37 :902-908.

733 Moojen DJF, Saris DBF, Auw Yang KG, Dhert WJA, Verbout AJ. The correlation and
734 reproducibility of histological scoring systems in cartilage repair. Tissue Eng 2002;8(4):627–
735 34.
736
737 Murphy CM, Haugh MG, O'Brien FJ. The effect of mean pore size on cell attachment,
738 proliferation and migration in collagen-glycosaminoglycan scaffolds for bone tissue
739 engineering. Biomaterials, 2010;31(3):461–466.
740
741 Murphy CM, Schindeler A, Gleeson JP, Yu NYC, Cantrill LC, Mikulec K, et al. A collagen–
742 hydroxyapatite scaffold allows for binding and co-delivery of recombinant bone
743 morphogenetic proteins and bisphosphonates. Acta Biomater. 2014;10 (5):2250-8.
744
745 Niederauer GG, Slivka MA, Leatherbury NC, Korvick DL, Harroff HH, Ehler WC, et al.
746 Evaluation of multiphase implants for repair of focal osteochondral defects in
747 goats. Biomaterials. 2000;21(24): 2561-2574.
748
749 O'Driscoll SW, Keeley FW, Salter RB, The chondrogenic potential of free autogenous periosteal
750 grafts for biological resurfacing of major full-thickness defects in joint surfaces under the

751 influence of continuous passive motion An experimental investigation in the rabbit, J Bone
752 Joint Surg. 1986;68(7):1017–1035
753
754 O'Shea TM, Xigeng M. Bilayered scaffolds for osteochondral tissue engineering. Tissue Eng.
755 Part B: Rev. 2008; 14(4): 447-464.
756
757 Orth P, Meyer HL, Goebel L, Eldracher M, Ong MF, Cucchiarini M, Madry H. Improved repair
758 of chondral and osteochondral defects in the ovine trochlea compared with the medial
759 condyle. J Orthop Res. 2013;31(11):1772-1779.
760
761 Patil S, Steklov N, Song L, Bae WC, D'Lima DD. Comparative biomechanical analysis of human
762 and caprine knee articular cartilage. Knee. 2014;21(1):119-25.
763
764 Pearce CJ, Gartner LE, Mitchell A, Calder JD. Synthetic osteochondral grafting of ankle
765 osteochondral lesions. Foot Ankle Surg. 2012;18(2):114-8.
766
767 Pek YS, Spector M, Yannas IV, Gibson LJ. Degradation of a collagen–chondroitin-6-sulfate
768 matrix by collagenase and by chondroitinase. Biomaterials. 2004;25(3):473-482.
769
770 Proffen BL, McElfresh M, Fleming BC, Murray MM. A comparative anatomical study of the
771 human knee and six animal species. Knee. 2012;19(4):493-9.
772
773 Quinlan E, Thompson E.M, Matsiko A, O'Brien FJ, López-Noriega A.
774 Functionalization of a collagen-hydroxyapatite scaffold with osteostatin to facilitate
775 enhanced bone regeneration, Advanced Healthcare Materials. 2015; (Accepted for
776 Publication). DOI: 10.1002/adhm.201500439
777
778 Raftery RM, Tierney EG, Curtin CM, Cryan SA, O'Brien FJ. Development of a gene-activated
779 scaffold platform for tissue engineering applications using chitosan-pDNA nanoparticles on
780 collagen-based scaffolds. J Control Release. 2015;210:84-94.
781

782 Rutgers M, van Pelt MJ, Dhert WJ, Creemers LB, Saris DB. Evaluation of histological scoring
783 systems for tissue-engineered, repaired and osteoarthritic cartilage. Osteoarthritis and
784 Cartilage Jan. 2010;18(1):12–23
785
786 Schneider CA, Rasband WS, Eliceiri KW. NIH Image to Image J: 25 years of image analysis, Nat
787 Methods, pp. 671, 2012
788
789 Sittinger M, Perka C, Schultz O, Häupl T, Burmester GR. Joint cartilage regeneration by tissue
790 engineering. Zeitschrift für Rheumatologie. 1999;58(3):130-135.
791
792 Tampieri A, Sandri M, Landi E, Pressato D, Francioli S, Quarto R et al. Design of graded
793 biomimetic osteochondral composite scaffolds. Biomaterials. 2008;29(26): 3539-3546.
794
795 Tierney CM, O'Brien FJ. Osteoblast activity on collagen-GAG scaffolds is affected by collagen
796 and GAG concentrations. J Biomed Mater Res A. 2009;91(1):92–101.
797
798 Tierney EG, Duffy GP, Cryan SA, Curtin CM, O'Brien FJ. Non-viral gene-activated matrices- next
799 generation constructs for bone repair. Organogenesis. 2013;19(1):22-28
800
801 van Susante JL, Buma P, Schuman L, Homminga GN, van den Berg WB, Veth RP. Resurfacing
802 potential of heterologous chondrocytes suspended in fibrin glue in large full-thickness defects
803 of femoral articular cartilage: an experimental study in the goat. Biomaterials.
804 1999;20(13):1167-1175.
805
806 Verhaegen J, Clockaerts S, Van Osch GJ, Somville J, Verdonk P, Mertens P. TruFit Plug for
807 Repair of Osteochondral Defects-Where Is the Evidence? Systematic Review of Literature.
808 Cartilage. 2015;6(1):12-9.
809
810 Zhou J, Xu C, Wu G, Cao X, Zhang L, Zhai Z, et al. *In vitro* generation of osteochondral
811 differentiation of human marrow mesenchymal stem cells in novel collagen-hydroxyapatite
812 layered scaffolds. Acta Biomater, 2011;7(11):3999–4006.
813

Figures:

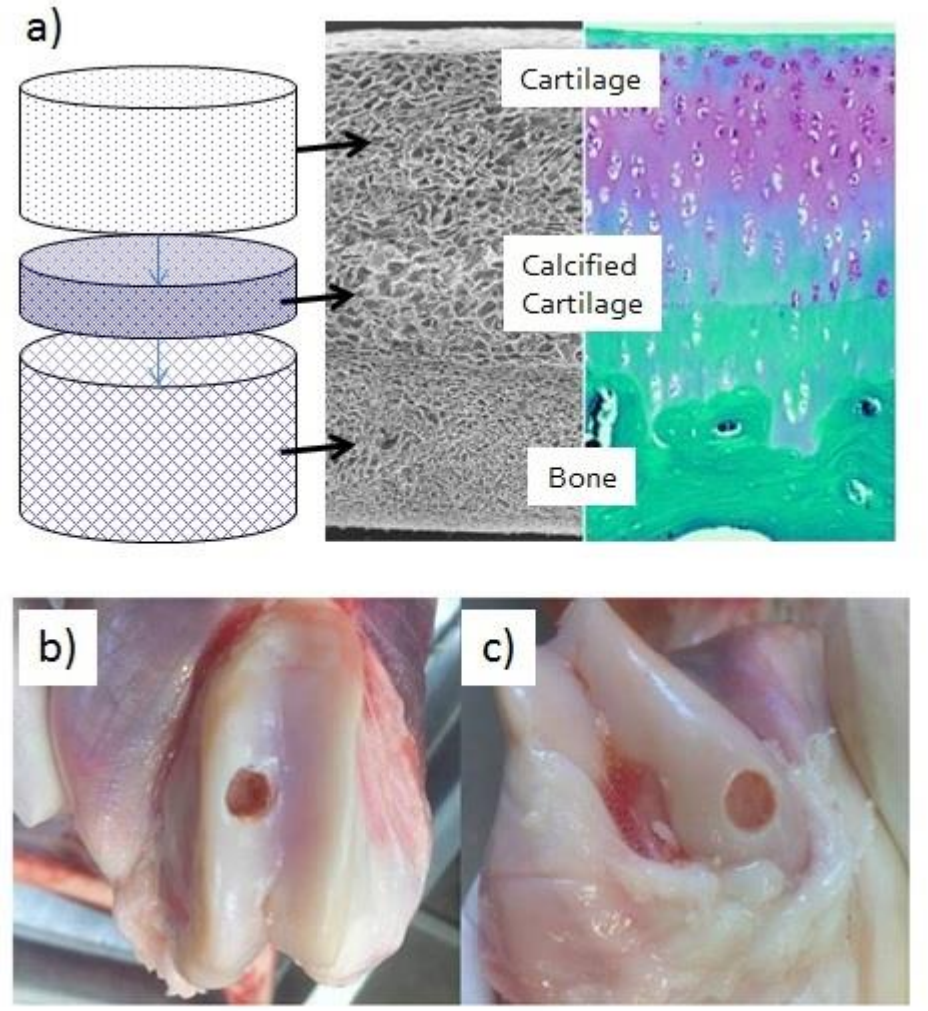

836

837 Figure 1: Multi-layered collagen-based scaffolds were implanted into defects in the goat stifle
838 joint. a) The scaffold has a porous microstructure with distinct but seamlessly integrated layer
839 designed specifically for the repair of bone, calcified cartilage and cartilage in an
840 osteochondral defect. Critically sized defects, 6 mm x 6 mm, were created in b) the lateral
841 trochlear ridge and c) the medial femoral condyle of the caprine stifle joints

842

843

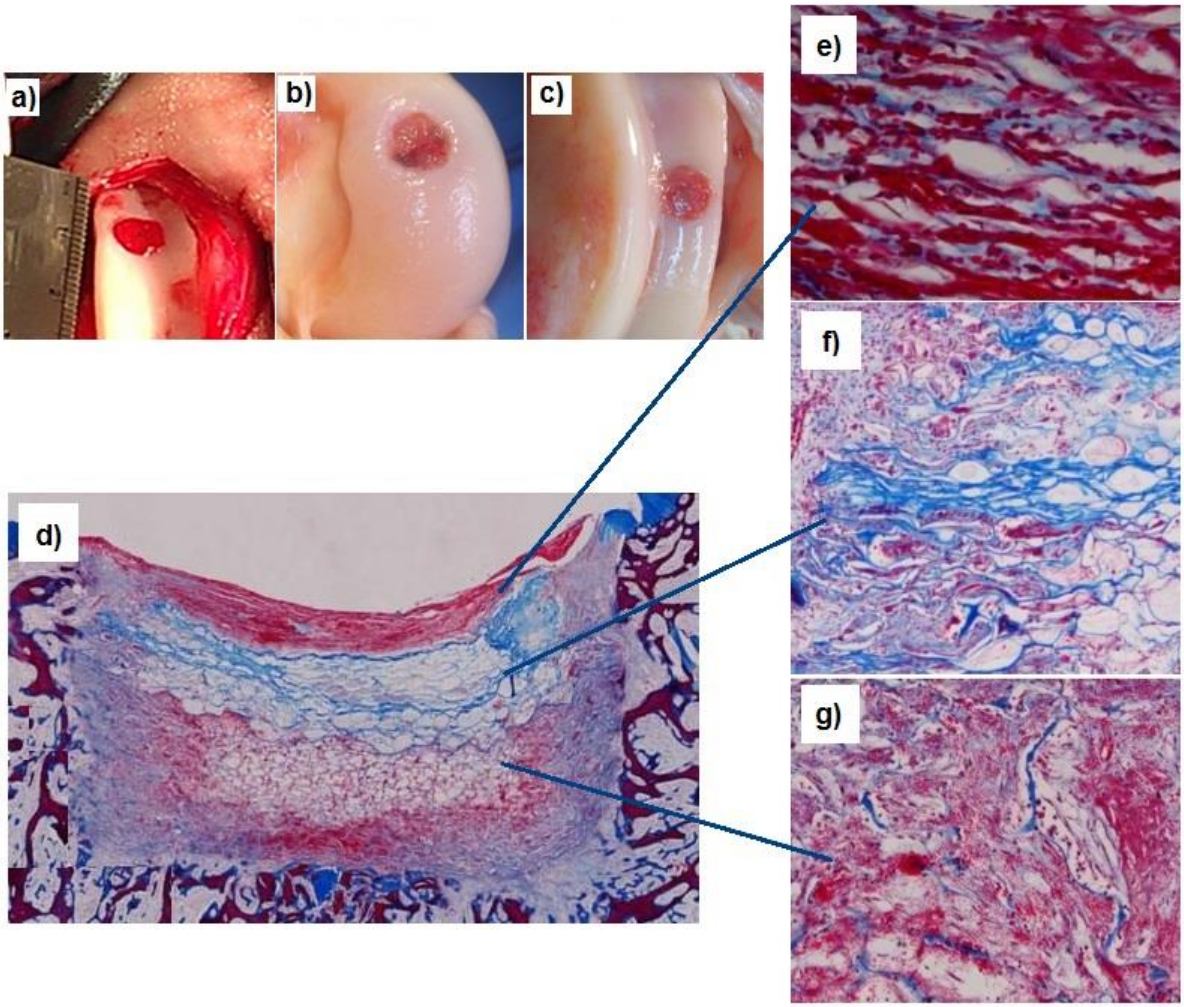

Figure 2: a) On implantation the scaffolds were seen to fill with blood and cells from the bone marrow. Macroscopic assessment at 2 weeks showed that the scaffolds were present within the medial condyle (b) and trochelar ridge (c) defect sites. d) Histological assessment (Masson's trichrome staining) showed cellular infiltration and early integration of repair tissue at 2 weeks post implantation in e) the cartilage layer, f) the intermediate layer and g) the bone layer of the multi-layered scaffold.

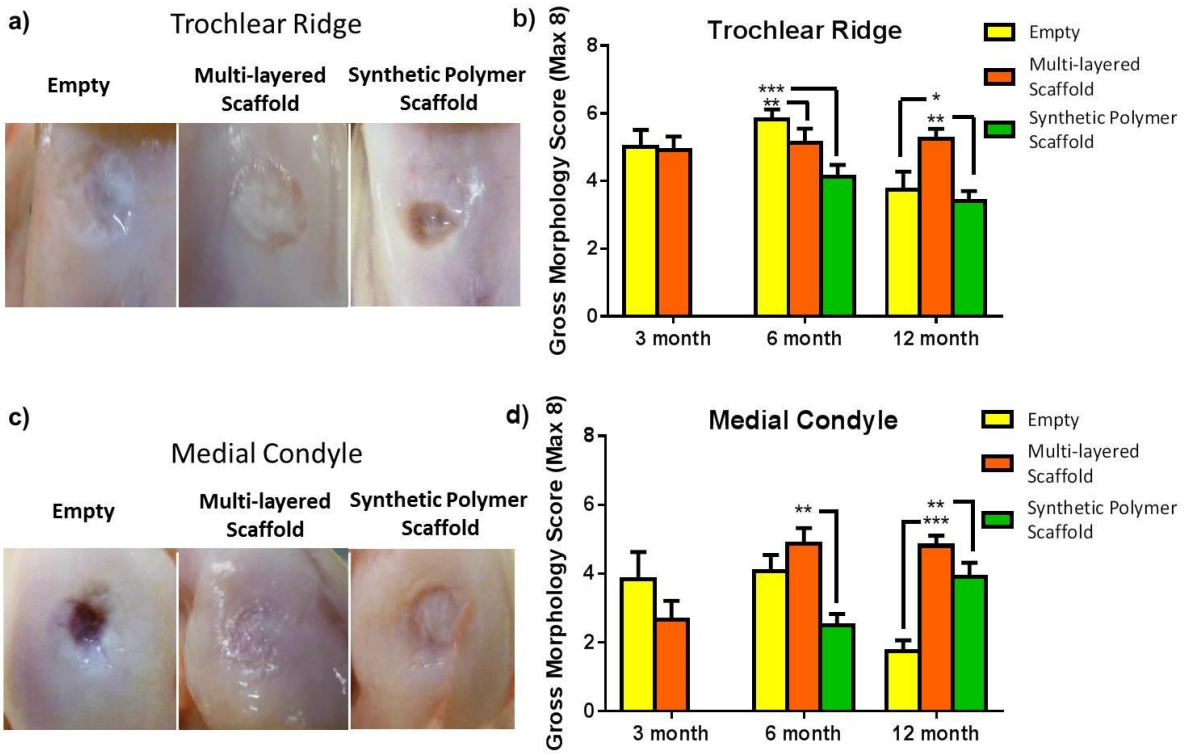

Figure 3: Gross morphology assessment of trochlear ridge (a,b) and medial condyle defects (c,d) at 3, 6 and 12 months. The defects treated with the multi-layered scaffold showed significantly higher gross morphology scores compared to the empty defects or the defects treated with the synthetic polymer scaffold. Representative macroscopic images show improved repair in the multi-layered scaffold group compared to the empty defect and synthetic polymer scaffold groups in b) the trochlear ridge and d) the medial condyle defect sites at 12 months. Statistical significant differences are represented as follows: * $p < 0.05$, ** $p < 0.01$, *** $p < 0.001$.

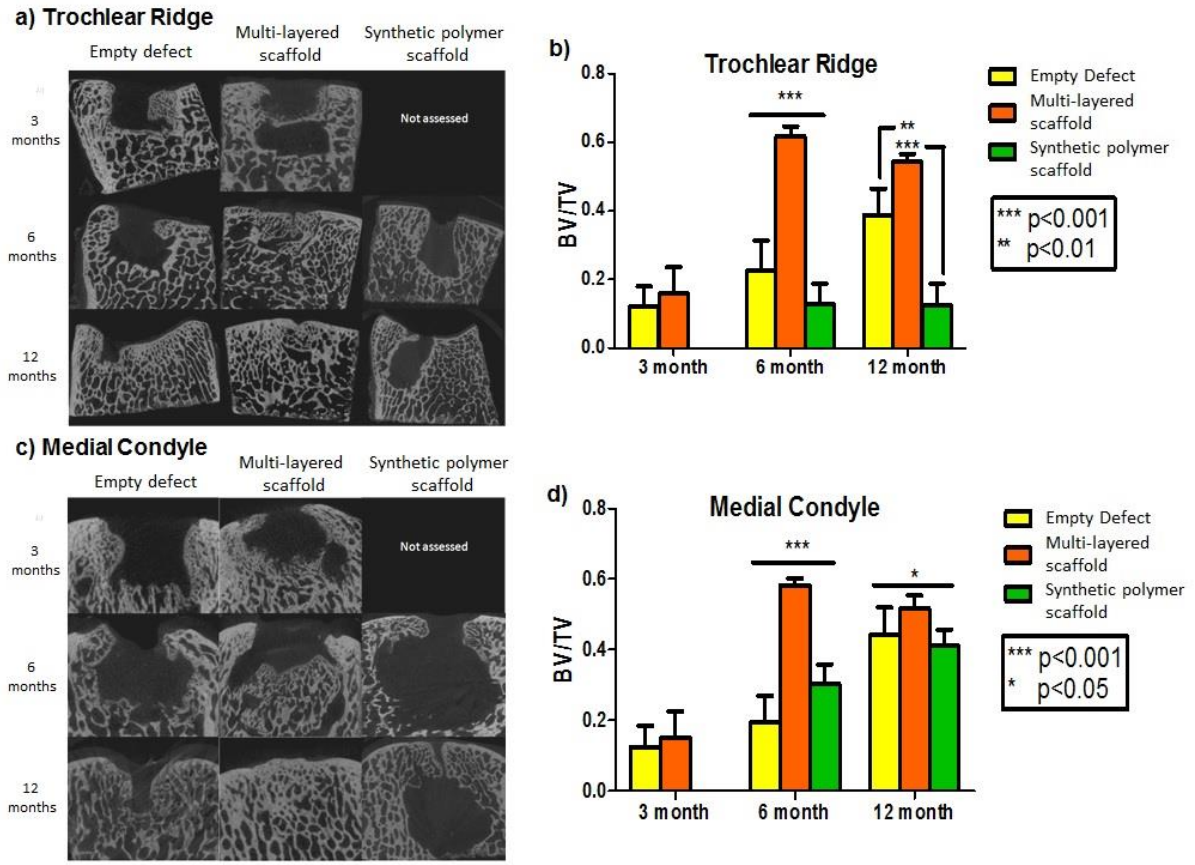

Figure 4: Micro-CT analysis showed improved subchondral bone repair in the multi-layered scaffold group. 2D projection images show the failure of subchondral bone restoration in the empty defect and synthetic polymer scaffold groups in a) the trochlear ridge and b) the medial femoral condyle. In comparison, the multi-layered scaffold group showed enhanced repair of subchondral bone. Quantitative micro-CT analysis of regenerated bone within the defect space demonstrates significantly greater level of bone formation in the multi-layered scaffold group compared to the other groups at 6 and 12 months post op (b,d). The values are expressed as mean ± standard deviation. Statistical significant differences are represented as follows: * $p < 0.05$, ** $p < 0.01$, *** $p < 0.001$.

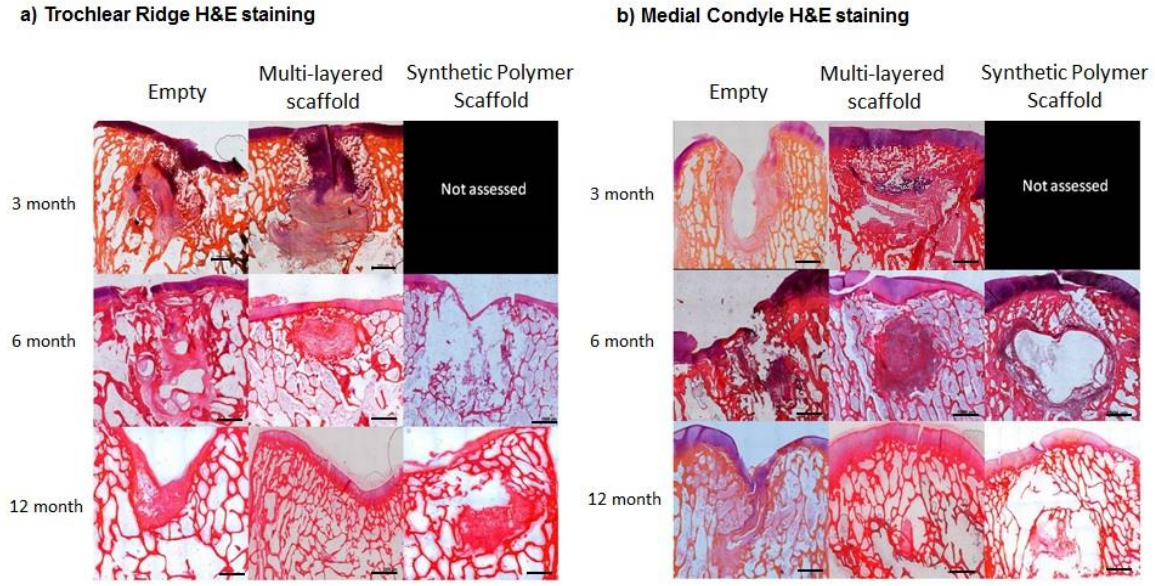

Figure 5: Histological staining (H&E) of the tissue repair in a) trochlear ridge and b) medial condyle at 3, 6 and 12 months post op. At 12 months, the empty group displays poor quality cartilage tissue and subchondral bone tissue, whereas the multi-layered scaffold group shows good quality cartilage and bone regeneration. Scale bar = 1000 µm

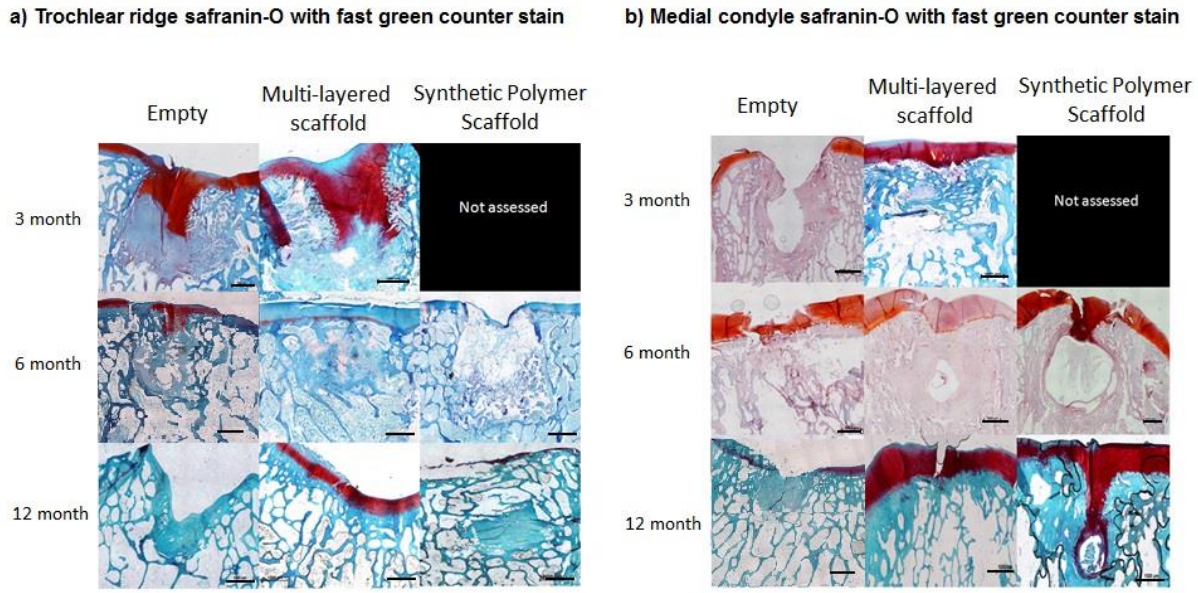

Figure 6: Histological staining (safranin-O) of a) the trochlear ridge and b) the medial condyle at 3, 6 and 12 months. The empty group and synthetic polymer scaffold groups display poor repair of cartilage and subchondral bone compared to the multi-layered scaffold group. Scale bar = 1000 µm

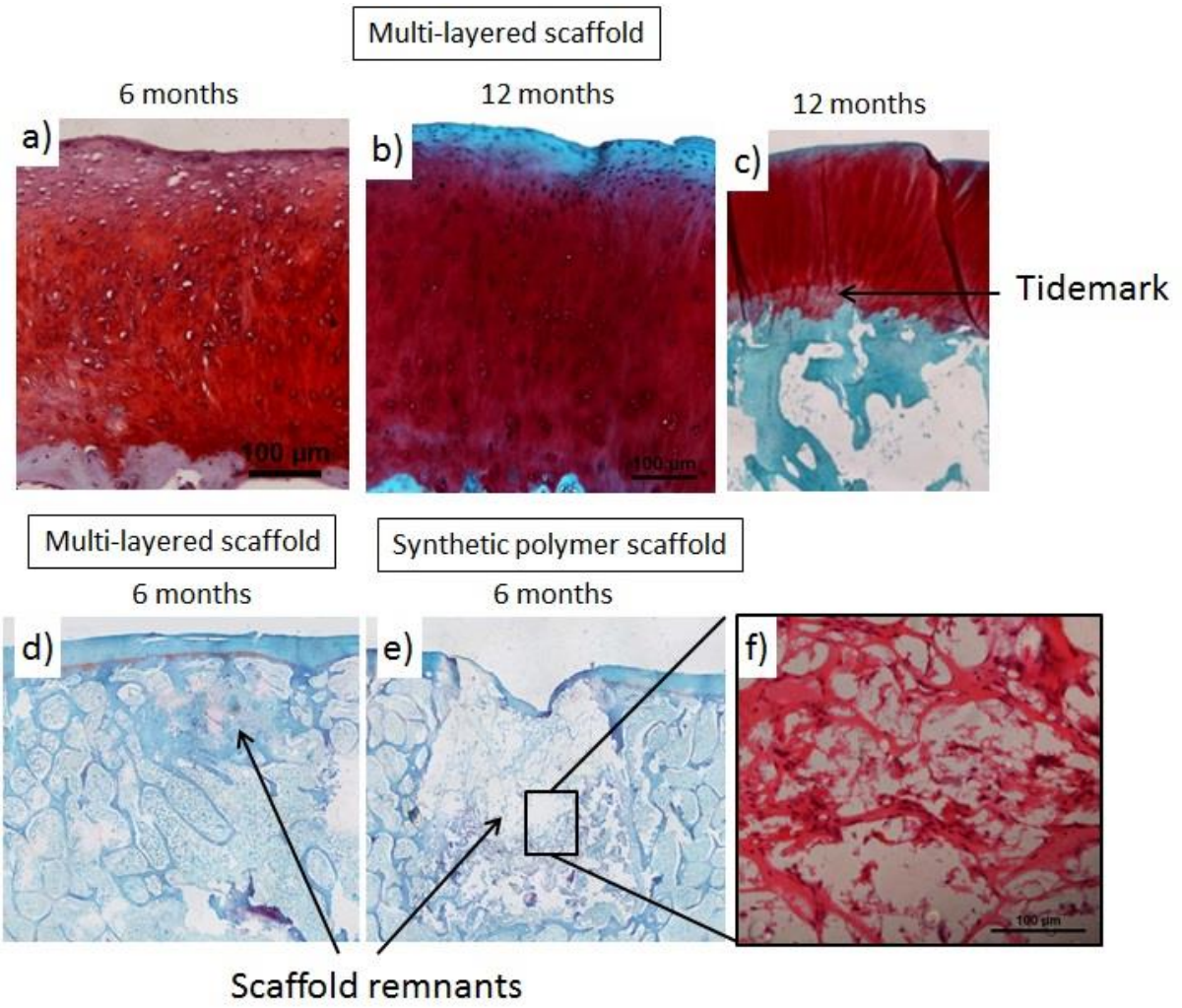

Figure 7: Histological analysis of repair tissue in the multi-layered scaffold group (safranin-O) at a) 6 months post op and b) 12 months post op. Fibrous-like repair tissue was observed at 6 months becoming more hyaline-like with intensive safranin-O staining by 12 months. Scaffolds degraded at different rates. The multi-layered scaffold was almost completed degraded by 6 months (d), whereas the synthetic polymer scaffold remained largely intact (e). Remnants of synthetic polymer scaffold are shown at higher magnification (H&E staining) (f). Scale bars represent 100 µm

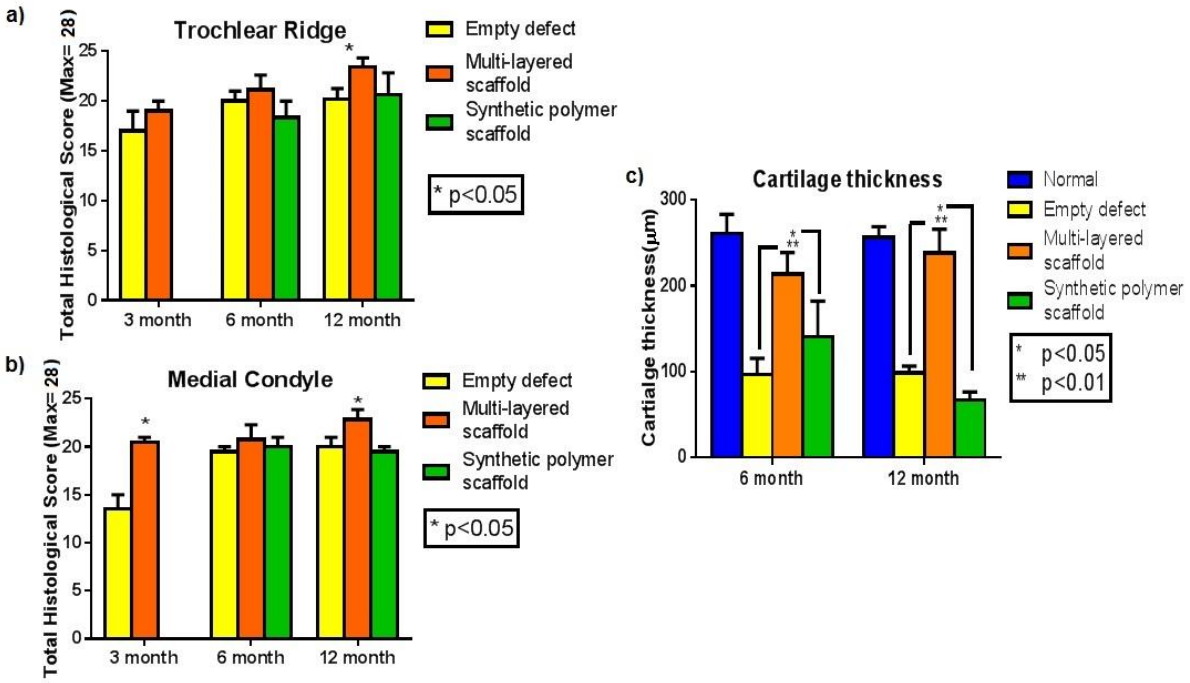

Figure 8: Total histology scores for a) the trochlear ridge and b) the medial condyle demonstrated improved tissue repair in the multi-layer scaffold group at 12 months post op. c) Cartilage thickness was quantified and found to be higher in the multi-layered scaffold group than in the empty defect and synthetic polymer scaffold groups at 6 and 12 months. Statistical significant differences are represented as follows: * $p < 0.05$, ** $p < 0.01$.

Tables:

Table 1: Study design showing the number of defects created in each group for osteochondral defect repair evaluation over a 12 month period. TR= trochlear ridge, MC= medial condyle.

Time point (months)	**Empty group (n)**		**Multi-layered scaffold group (n)**		**Synthetic polymer scaffold group (n)**	
Defect site	TR	MC	TR	MC	TR	MC
2 weeks	-	-	2	2	-	-
3	3	3	3	3	-	-
6	4	4	7	7	3	3
12	6	6	7	7	3	3

Table 2: Gross morphology scoring system for cartilage repair. Maximum score possible score is 8

Characteristic	**Grading**	**Score**
Edge integration (new tissue relative to native cartilage)	Full	2
	Partial	1
	None	0
Smoothness of cartilage surface	Smooth	2
	Intermediate	1
	Rough	0
Cartilage surface, degree of filling	Flush	2
	Slight depression	1
	Depressed/overgrown	0

Colour of cartilage, opacity or translucency of the neocartilage	Opaque	2
	Translucent	1
	Transparent	0

Table 3: Modified histological scoring system for cartilage repair. Maximum score possible is 28

Characteristic	**Grading**	**Score**
I. Nature of predominant cartilage tissue	Hyaline cartilage	4
	Mostly hyaline cartilage	3
	Mixed hyaline and fibrocartilage	2
	Mostly fibrocartilage	1
	Mostly fibrocartilage and non-chondrocytic cells	0
II. Structural Characteristics		
A. Surface regularity	Smooth and intact	3
	Superficial horizontal lamination	2
	Fissures	1
	Severe disruption, including fibrillation	0
B. Structural Integrity	Normal	2

	Slight disruption, including cysts	1
	Severe disintegration	0
C. Thickness	100% of normal adjacent cartilage	2
	50-100% of normal cartilage	1
	0-50% of normal cartilage	0
D. Bonding to adjacent cartilage	Bonded at both ends of graft	2
	Bonded at one end or partially at both ends	1
	Not bonded	0
III. Freedom from cellular changes of degeneration		
A. Hypocellularity	Normal cellularity	2
	Slight hypocellularity	1
	Moderate hypocellularity or hypercellularity	0
B. Chondrocyte clustering	No clusters	2
	< 25% of the cells	1
	25-100% of the cells	0
IV. Freedom from degradation changes in articular cartilage		
A. Freedom from degenerative changes in adjacent cartilage	Normal cellularity, no clusters, normal staining	3
	Normal cellularity, mild clusters, moderate staining	2
	Mild or moderate hypocellularity, slight staining	1
	Severe hypocellularity, poor or no staining	0
V. Reconstitution of subchondral bone		
A. Reconstitution of subchondral bone	Normal	3
	Reduced subchondral bone reconstitution	2
	Minimal subchondral bone reconstitution	1
	No subchondral bone reconstitution	0
	None/mild	2

B. Inflammatory response in subchondral bone region	Moderate	1
	Severe	0
VI. Safranin-O staining	Normal	3
	Moderate	2
	Slight	1
	None	0
Total maximum score		**28**

943

944